Improving Load Estimates for NO$_3$ and P in Surface Waters by Characterizing the Concentration Response to Rainfall Events

JOACHIM C. ROZEMEIJER,*,†,‡,¶ YPE VAN DER VELDE,§,‡,¶ FRANS C. VAN GEER,⊥,† GERRIT H. DE ROOIJ,|| PAUL J. J. F. TORFS,§ AND HANS PETER BROERS‡,⊥

Department of Physical Geography, Utrecht University, P.O. Box 80125, NL-3508 TC Utrecht, The Netherlands, Soil Physics, Ecohydrology and Groundwater Management Group, Wageningen University, P.O. Box 47, NL-6700 AA Wageningen, The Netherlands, Groundwater and Subsurface Department, Deltares, P.O. Box 85467, NL-3508 AL Utrecht, The Netherlands, TNO Geological Survey of The Netherlands, P.O. Box 80015, 3508 TA, Utrecht, The Netherlands, and Department Soil Physics, Helmholtz Centre for Environmental Research, Theodor-Lieser-Strasse 4, D-06120 Halle, Germany

For the evaluation of action programs to reduce surface water pollution, water authorities invest heavily in water quality monitoring. However, sampling frequencies are generally insufficient to capture the dynamical behavior of solute concentrations. For this study, we used on-site equipment that performed semicontinuous (15 min interval) NO$_3$ and P concentration measurements from June 2007 to July 2008. We recorded the concentration responses to rainfall events with a wide range in antecedent conditions and rainfall durations and intensities. Through sequential linear multiple regression analysis, we successfully related the NO$_3$ and P event responses to high-frequency records of precipitation, discharge, and groundwater levels. We applied the regression models to reconstruct concentration patterns between low-frequency water quality measurements. This new approach significantly improved load estimates from a 20% to a 1% bias for NO$_3$ and from a 63% to a 5% bias for P. These results demonstrate the value of commonly available precipitation, discharge, and groundwater level data for the interpretation of water quality measurements. Improving load estimates from low-frequency concentration data just requires a period of high-frequency concentration measurements and a conceptual, statistical, or physical model for relating the rainfall event response of solute concentrations to quantitative hydrological changes.

* Corresponding author phone: +31-30-2564724; fax: +31-30-2564855; e-mail: joachim.rozemeijer@deltares.nl.
† Utrecht University.
‡ Deltares.
§ Wageningen University.
⊥ TNO-Geological Survey of The Netherlands.
|| Helmholtz Centre for Environmental Research.
¶ Both authors (Joachim and Ype) can be considered the first author of this paper.

Introduction

Surface water pollution is a serious problem in areas with intensive agriculture such as The Netherlands (*1*). Policy makers of the European Union and elsewhere in the world aim at improving water quality in receiving surface water bodies (e.g., ref *2*). For the evaluation of action programs and pilot studies, water authorities invest heavily in the monitoring of NO$_3$ and P loads from upstream catchments. However, the interpretation of the data from their monitoring networks is often problematic. Grab samples only provide 'snapshots' of solute concentrations, and sampling frequencies are generally not sufficient to capture the dynamic behavior of surface water quality (*3–5*). Together with the uncertainties in the concentration measurements themselves (e.g., ref *6*), this results in large uncertainties in the estimates of loads and average concentrations.

The uncertainties in estimates of loads and average concentrations can be reduced by increasing the sampling frequencies. However, the field sampling, sample transport, and laboratory procedures are laborious and expensive. Another option is to apply on-site automatic samplers and analyzers, which can produce continuous concentration time series of many chemicals (e.g., refs *5* and *7*). Major drawbacks of this equipment are the expensive purchase, maintenance, and field installation in a sheltered environment with electrical power supply. Furthermore, the complex automatic analyzers are vulnerable to technical problems and power supply failures. As a consequence, regional surface water quality monitoring will continue to rely predominantly on low-frequency grab sampling data. Therefore, improving load estimates from low-frequency concentration measurements is still an important research topic.

A favorable approach for improving load estimates from low-frequency concentration data is to make use of the explanatory strength of commonly available continuous measurements of quantitative hydrological data like precipitation, discharge, and groundwater levels. These measurements are relatively inexpensive and often already available near surface water quality monitoring locations to facilitate quantitative water management such as flood control and groundwater level management.

Previous studies focused primarily on the use of long-term concentration-discharge relations to improve load estimates from low-frequency concentration data. However, in several comparison studies, none of the methods clearly outperformed the methods that were based on simple linear or stepwise interpolation (e.g., refs *8* and *9*). The main obstacle is the poorly understood nonstationary behavior of the concentration-discharge relationships. Especially in smaller catchments, event-scale concentrations-discharge relations are highly solute- and catchment-specific, show hysteresis, and change during the year (e.g., refs *7*, *10*, and *11*).

In recent studies, high-frequency measurements have increased the understanding of short-scale variations of solute concentrations in surface water (*7*, *12*). For example, several researchers reported peaks in P-concentrations in response to rainfall events (*13*, *14*). The NO$_3$ response to rainfall events depends on the hydrogeochemical properties of the catchment; some authors observed a lowering of concentrations (*10*, *15*, *16*), while others detected concentration peaks in response to events (*17–19*). The new understanding of short-scale variations in water quality has not yet been applied for improved methodologies for estimating loads from low-frequency concentration data.

This study aimed at improving load estimates from low-frequency concentration measurements by reconstructing the responses of NO_3 and P concentrations to rainfall events using commonly available quantitative hydrological data. We present a unique year-round combined data set of semicontinuous (15 min interval) measurements of NO_3 and P concentrations, discharge, precipitation, and groundwater levels. Through a sequential multiple regression analysis, we related variables describing the water quality rainfall event responses to variables describing the hydrological responses. We applied these relations to reconstruct concentration patterns between low-frequency grab sample measurements, which significantly improved estimates of annual loads.

Methods

Study Area and Field Measurements. We installed a multiscale experimental setup in the Hupsel catchment (6.64 km²) in the eastern part of The Netherlands (52°03′ N; 6°38′ E). This catchment was selected because of the dominance of agricultural land use, the dense artificial drainage network, and the absence of point sources and water inlet from outside the catchment. A detailed description of the Hupsel catchment and of all installations and measurements is given in ref *20*. For this study, semicontinuous records of NO_3 and P concentrations and discharge were collected at the catchment outlet from June 2007 to July 2008. For the semicontinuous NO_3 concentration measurements we used a Hydrion-10 multiparameter probe (Hydrion BV, Wageningen, The Netherlands). Semicontinuous measurements of dissolved-P (ortho-P) and total-P concentrations were performed by a Sigmatax sampler and a Phosphax Sigma autoanalyzer (both Hach Lange GmbH, Düsseldorf, Germany). See the Supporting Information (pp S3−S4) and ref 7 for a more detailed description of this equipment. The NO_3 concentration values in this paper are given in milligrams nitrate per liter (mg NO_3 · L^{-1}). For P, we focused our analyses on the total-P concentrations which are given in milligrams total-phosphorus per liter (mg P-tot · L^{-1}).

In addition to the automatic solute concentration measurements, we collected weekly grab samples from the catchment outlet. These weekly measurements were used to correct for the potential drift and offset of the continuous concentration measurements. The stream discharge at the catchment outlet was recorded every 15 min using a calibrated weir. Precipitation and groundwater levels were measured for the same period at an experimental field within the catchment.

Event-Response Characterization. The event responses of NO_3 and P concentrations, discharge, and groundwater levels were analyzed through a set of event-response characteristics (Table 1), which will be discussed in this section. For the quantitative hydrological data, we deduced as many characteristics as possible in order to let the subsequent statistical modeling decide which characteristics contain the most relevant explanatory information for characterizing the NO_3 and P concentration response. First, we defined selection criteria for events, based on the continuous discharge records. We selected all events with a maximum discharge above 100 $L \cdot s^{-1}$ (1.3 mm·d^{-1}), a discharge increase of at least 20 $L \cdot s^{-1}$ (0.26 mm·d^{-1}), and a discharge decrease after the maximum of at least 20 $L \cdot s^{-1}$. Less pronounced events generally did not significantly affect the load estimates, because the NO_3 and P concentrations did not respond. When varying rainfall intensities caused two discharge peaks to occur within 6 h, these peaks were merged into one event. The start time of an event was defined as the first moment with a 5% discharge increase within 2 h, leading up to a discharge peak.

The events with uninterrupted records of precipitation, discharge, groundwater levels, and NO_3 or P concentrations

were selected for further analysis. These rainfall events were characterized by the total rainfall amount (*Rtot*), the maximum rainfall intensity (*RImax*), and the Antecedent Precipitation and Evaporation Index (*APEI*) (Table 1). The *APEI* is a frequently used measure for the initial wetness of the catchment at the onset of the rainfall event. We derived the *APEI* from precipitation and evaporation data, following the method described by Fedora and Beschta (*21*). The Makkink relation (*22*) was applied to estimate evapotranspiration using temperature and net incoming radiation data from the weather station within the Hupsel catchment.

The NO_3 and P concentration responses to the rainfall events were described by three event-response characteristics: the maximum concentration change, the time to maximum concentration change, and the recovery time. A graphical explanation of these response characteristics is given in Figure 1. The maximum NO_3 concentration change during events (*rdN*) is described as a percentage of the starting concentration (*Ns*). For P, the starting concentrations (*Ps*) were very low relative to the peak concentrations (*Pmax*). Therefore, absolute P concentration changes (*dP*) were more appropriate for characterizing the P concentration responses to events. The times to maximum change for NO_3 (*TdN*) and P (*TdP*) are defined as the time interval between the start of the event and the moment of maximum change. The concentration recovery time is determined by fitting an exponential recovery curve to the measured concentrations for the first 24 h after the time of maximum concentration change. The concentration recovery is described by

$$Rec(t) = e^{-t/T_{rec}} \qquad (1)$$

where $Rec(t)$ [-] is the relative recovery of the concentration or discharge at time t when $t = 0$ represents the start of the recovery or the time of maximum change. The recovery time T_{rec} [T] for NO_3 is denoted by *TNrec* and for P by *TPrec*. The values for the total loads (*LN* and *LP*) were calculated for the period between the start of the event until the time of 50% recovery of the discharge or until the start of the next event.

To characterize the discharge and groundwater level event responses, we derived the same response characteristics as described for the concentrations in the previous section (see also Table 1). In addition, we determined the average and the maximum discharge slope (*SQ* and *SQmax*) as well as the time to the maximum discharge slope (*TSQmax*). We also derived the average and the maximum slope of the groundwater levels (*SG* and *SGmax*).

Furthermore, we calculated a time series of the proportion of quick-flow from the continuous discharge records. For this, we used the hydrograph separation method described by Hewlett and Hibbert (*23*), with a constant separation slope of 0.2 $L \cdot h^{-2}$. With this relatively low slope value, 100% base-flow conditions only occur after extended dry periods, and a uniform distribution of quick-flow proportions over time was achieved. For each event, we determined the quick-flow percentage at the start of the event (*QFs*), the maximum quick-flow percentage (*QFmax*), and the maximum change in quick-flow percentage during the event (*dQF*).

Regression Analysis. We first applied a singular linear regression analysis between all NO_3 and P concentration response characteristics and all quantitative hydrological event characteristics. This analysis gives an overview of the quantitative hydrological characteristics that can explain part of the variation in the NO_3 and P response characteristics to rainfall events.

Subsequently, a sequential multiple linear regression analysis was conducted. We excluded the data of March 1 to April 3, 2008 for this analysis, because we selected this period for the validation of the event-response models. This period was chosen for validation because ten major and minor

TABLE 1. Summary of the Event Characteristics That Were Derived from the Continuous Measurements of the Rainfall Events That Were Analyzed in This Study

rainfall characteristics	short	unit	mean	median	st. dev.
total rainfall	$Rtot$	mm	10.1	9.3	5.4
maximum rainfall intensity	$RImax$	mm h^{-1}	3.3	2.8	2.4
antecedent precipitation and evaporation index	$APEI$	-	17.4	15.1	10.1

NO_3 characteristics	short	unit	mean	median	st. dev.
NO_3 concentration at start of event	Ns	mg L^{-1}	44.3	42.4	11.1
NO_3 minimum concentration during event	$Nmin$	mg L^{-1}	27.6	26.5	10.0
NO_3 relative concentration change during event	rdN	%	37	37	18
time to maximum NO_3 concentration change	TdN	h	8.6	8.4	3.9
recovery time NO_3	$TNrec$	h	11.4	10.6	5.9
NO_3 total load	LN	kg	980	839	638

P characteristics	short	unit	mean	median	st. dev.
P concentration at start of event	Ps	μg L^{-1}	0.15	0.10	0.14
P maximum concentration during event	$Pmax$	μg L^{-1}	0.94	0.77	0.89
P concentration change during event	dP	μg L^{-1}	0.85	0.66	0.89
time to maximum NO_3 concentration change	TdP	h	6.8	5.0	5.4
recovery time P	$TPrec$	h	6.1	5.5	4.0
P total load	LP	kg	4.2	3.3	3.5

discharge characteristics	short	unit	mean	median	st. dev.
discharge at start of event	Qs	L s^{-1}	0.15	0.10	0.14
maximum discharge during event	$Qmax$	L s^{-1}	0.42	0.34	0.31
discharge change during event	dQ	L s^{-1}	0.27	0.21	0.24
time to maximum discharge change	TdQ	h	11	10	6
average slope rising discharge	SQ	L s^{-1} h^{-1}	0.030	0.019	0.035
maximum slope rising discharge	$SQmax$	L s^{-1} h^{-1}	0.074	0.045	0.074
time to maximum discharge slope	$TSQmax$	h	6	5	4
recovery time discharge	$TQrec$	h	49	30	42
total discharge	$Qtot$	m^3	8757	6963	5461
quick-flow percentage at start of event	QFs	%	36	42	31
maximum quick-flow percentage during event	$QFmax$	%	77	80	18
quick-flow percentage change during event	dQF	%	41	37	27

groundwater level characteristics	short	unit	mean	median	st. dev.
groundwater level below surface at start of event	Gs	cm	54	57	22
maximum groundwater level during event	$Gmax$	cm	35	33	17
groundwater level change during event	dG	cm	20	18	12
average slope rising groundwater level	SG	cm/h	1.7	1.8	1.3
maximum slope rising groundwater level	$SGmax$	cm/h	5.7	5.8	3.5

rainfall events affected the NO_3 and P concentrations and because our continuous time series were not interrupted by technical failures. The sequential regression analysis started
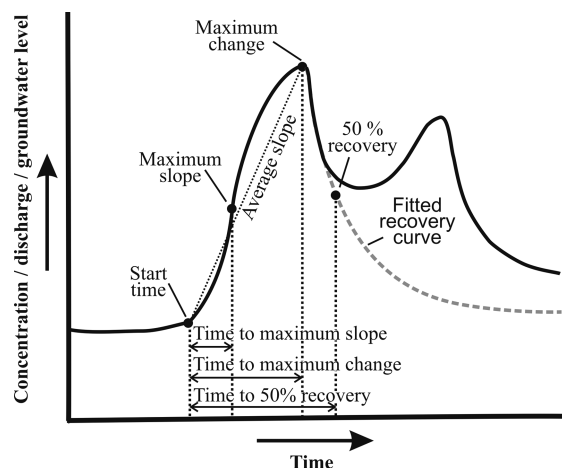

FIGURE 1. Graphical explanation of several rainfall event-response characteristics. See the main text for an explanation.

with selecting the singular regressions with the highest coefficient of determination (R^2) for explaining the NO_3 and P response characteristics. Subsequently, we searched for the best regression with two explanatory variables. This regression was selected whenever the R^2 was at least 5% higher than the singular regression model. In the final step, we searched for the best regression model with three explanatory variables. Again, this model was only selected when the R^2 was 5% higher than the model with two explanatory variables. The selected event-response models were validated using the data of the rainfall events during the validation period.

Load Estimates. We first estimated the NO_3 and P loads for the validation period of March 1 to April 3, 2008. To reconstruct the NO_3 and P concentration patterns, we used our weekly samples for describing the base level concentrations and our event-response models for describing the concentration changes during rainfall events. The base level concentrations were reconstructed by a LOWESS smooth interpolation (24) through our grab sample measurements during low flow conditions (<100 L·s^{-1} or 1.3 mm·d^{-1}). The concentration changes during events were reconstructed by the event-response models, using the quantitative hydrological event-response characteristics from Table 1. We
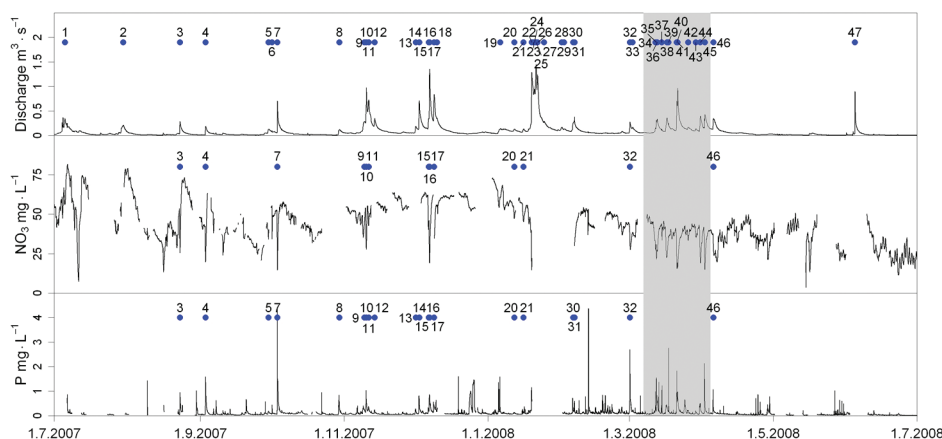
FIGURE 2. Graphs of the measured discharge and NO$_3$ and P concentrations from July 2007 until July 2008. The rainfall events marked in the NO$_3$ and P graphs were selected for further analysis; they occurred outside the validation period (indicated in gray) and have uninterrupted concentration time series.
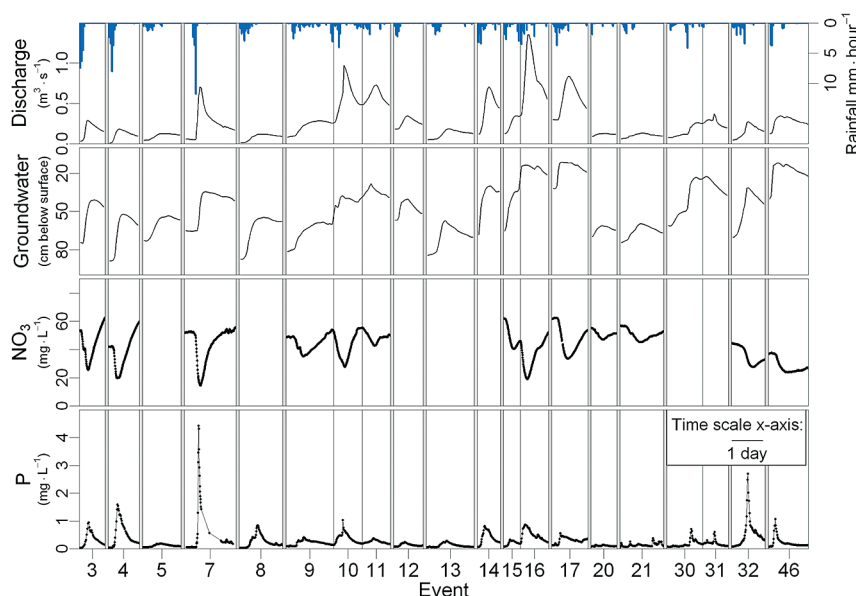

FIGURE 3. Responses of discharge, groundwater levels, and NO$_3$ and P concentrations to the selected rainfall events. The event numbers correspond to the numbers in Figure 2.

estimated the NO$_3$ and P loads from the reconstructed concentrations and the continuous discharge records. For comparison, we also calculated the 'true' loads based on our continuous concentration measurements. In addition, NO$_3$ and P loads were estimated from the interpolated concentrations without a concentration reconstruction during events. This represented a common load estimate from low-frequency grab sampling data.

As a next step, we applied the same concentration reconstruction procedure to estimate the total annual NO$_3$ and P loads. Again, we compared the load estimate from our reconstruction approach with a common load estimate without reconstruction and to the 'true' load estimate from the continuous concentration measurements. Note that our continuous concentration time series were interrupted for a few periods due to technical failures. For a fair comparison between the different load estimates, these missing data periods were excluded. However, we also made a best estimate of the total annual NO$_3$ and P loads. This was achieved by using our concentration reconstruction approach to fill in the data gaps in our continuous time series of NO$_3$ and P concentrations.

Results

Field Measurements and Event Characteristics. In total, 47 precipitation-discharge events occurred in the period from June 2007 until July 2008. Figure 2 shows the total time series of measured discharges and the NO$_3$ and P concentrations. We selected all events with complete continuous data records and excluded the events during the validation period from March 1 until April 3. From the 47 events, 13 events were selected for NO$_3$ and 20 events for P. The selected events are indicated by dots in the NO$_3$ and P concentration graphs in Figure 2. During the 13 selected events for NO$_3$, 18% of the annual rainfall occurred, while 14% of the annual discharge and 13% of the annual NO$_3$ load were registered. During the 20 selected events for P, 25% of the annual rainfall, 18% of the annual discharge, and 34% of the annual P load were registered.

The responses of discharge, groundwater levels, and NO$_3$ and P concentrations to the selected rainfall events are shown in Figure 3. From this figure, the short-term concentration responses to the events appear to be consistent throughout the year. The NO$_3$ concentrations repetitively show a temporal decrease in response to events. The total-P concentrations, which are generally very low, react to the events with a short

TABLE 2. Results of the Sequential Multiple Regression Analysis—the Best Event-Response Models for Explaining the NO_3 and P Responses to Rainfall Events from Quantitative Hydrological Event Characteristics[a]

	intercept	independent or explanatory variables			R^2
		no. 1	no. 2	no. 3	
		NO_3 Event-Response Models			
rdN (%)	0.11	dQ (0.30)	SG (0.084)		0.95
TdN (h)	29.9	TSQmax (1.14)	Log(dQ) (2.84)	QFmax (−29.2)	0.85
TNrec (h)	29.2	RImax (−1.63)	QFs (−4.6)	Gmax (0.15)	0.86
		P Event-Response Models			
dP (mg·L^{-1})	0.17	RImax (0.24)	APEI (−0.024)	1/TQrec (17.0)	0.77
TdP (h)	10.82	TQrec (−0.0042)	TdQ (0.87)	QFmax (−14.2)	0.74
TPrec (h)	1.89	SQmax (−79.5)	Rtot (0.45)	Qmax (20.3)	0.82

[a] The numbers between brackets are the parameter values belonging to the independent variable. For example, the response model for the relative changes in NO_3 concentrations in response to rainfall events: rdN = 0.11 + 0.30 dQ + 0.084 SG.
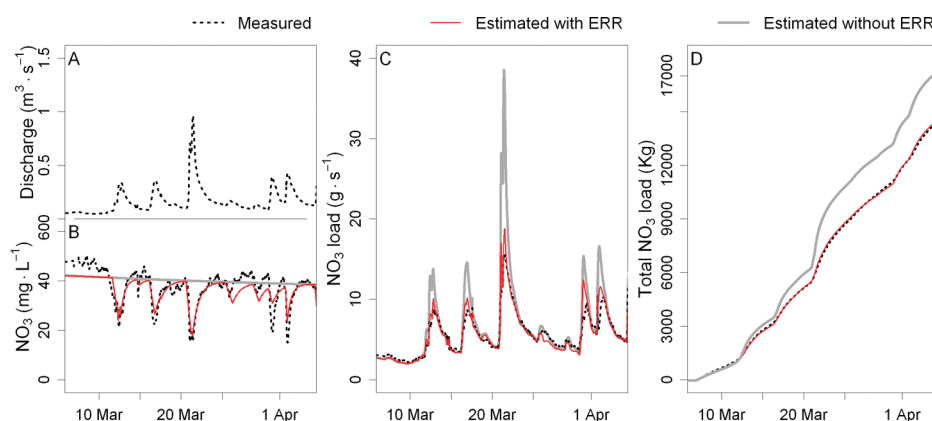

FIGURE 4. Results for NO_3 for the validation period from March 1 to April 3, 2008; the discharge records (A), the measured NO_3 concentrations, the moving average through the grab sampling measurements (without event response reconstruction, ERR), and concentrations with event response reconstruction (ERR) (B), the measured and reconstructed NO_3 loads (C), and the cumulative measured and reconstructed NO_3 loads (D).

and sudden increase. The summary statistics of the response characteristics are given in Table 1. The event characteristics show that our data set covers a wide range of event properties and antecedent conditions.

Regression Analysis and Load Estimates. Table 2 gives the best event-response models from the sequential multiple regression analysis. The coefficient of determination (R^2) for the NO_3 and P response characteristics varies from 74% for TdP up to 95% for rdN. The singular linear regression results as well as measured-versus-modeled verification graphs of the multiple regression models are given in the Supporting Information.

The event-response models from Table 2 were applied to reconstruct the NO_3 and P concentration pattern for the validation period of March 1 to April 3, 2008. The reconstructed concentration patterns are shown in Figure 4b for NO_3 and 5b for P. These figures also present the actual, continuously measured concentrations and the LOWESS interpolation through our weekly grab sampling concentration measurements. The load estimates based on our reconstructed concentration patterns are shown in Figures 4c and 5c. Cumulative load estimates are given in Figures 4d and 5d. The total measured loads for 1 March to 3 April 2008 were 121 kg for P and 14.0 × 10³ kg for NO_3. The moving average interpolation through the low-frequency grab samples underestimated the measured P load by 63% and overestimated the measured NO_3 load by 20%. The event response reconstruction method underestimated the P load by 5% and overestimated the NO_3 load by 1%.

The results for the total annual load estimates for NO_3 and P are shown in Figure 6. The measured annual loads,

without the missing data periods, were 448 kg for P and 86.1 × 10³ kg for NO_3. The LOWESS interpolation through the low-frequency grab samples underestimated the P load by 60% and overestimated the measured NO_3 load by 8%. The event response reconstruction method underestimated the P load by 4% and underestimated the NO_3 load by 3%. The best estimates of the total annual loads for the Hupsel catchment, including the reconstructions for the missing data periods, came to 570 kg for P (0.27 kg·ha^{-1}) and 121 ·10³ kg for NO_3 (41 kg·ha^{-1}).

Discussion and Implications

In this study, we successfully improved load estimates from low-frequency NO_3 and P concentration measurement using the explanatory strength of generally available and inexpensive quantitative hydrological data. Previously proposed methods to achieve this did not outperform standard interpolation methods (e.g., refs 8 and 9). We related the rainfall event responses of NO_3 and P concentrations to precipitation records and to the responses of discharge and groundwater levels. These relations were used to improve the load estimates for our validation period from a 20% to a 1% bias for NO_3 and from a 63% to a 5% bias for P. Our results demonstrate that the interpretation of water quality measurements can be improved by using the explanatory strength of commonly available precipitation, discharge, and groundwater level measurements.

The foundation of this new approach to improve load estimates was a unique data set of year-round continuous NO_3 and P measurements combined with continuous
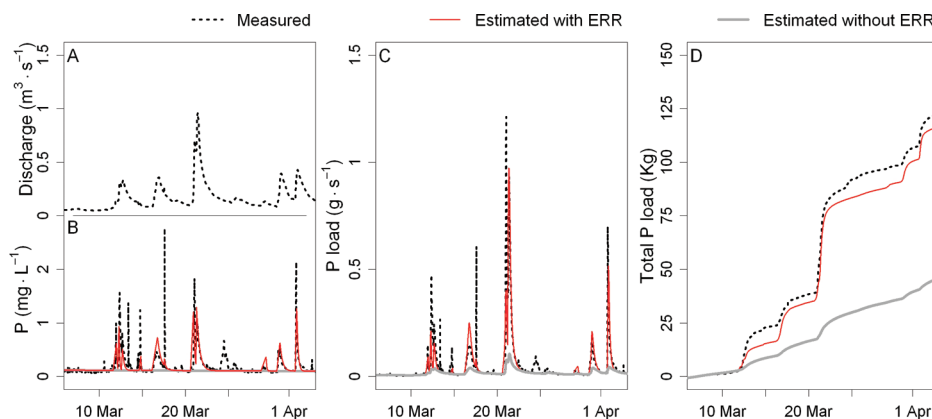
FIGURE 5. Results for P for the validation period from March 1 to April 3, 2008; the discharge records (A), the measured P concentrations, the moving average through the grab sampling measurements (without event response reconstruction, ERR), and concentrations with event response reconstruction (ERR) (B), the measured and reconstructed P loads (C), and the cumulative measured and reconstructed P loads (D).
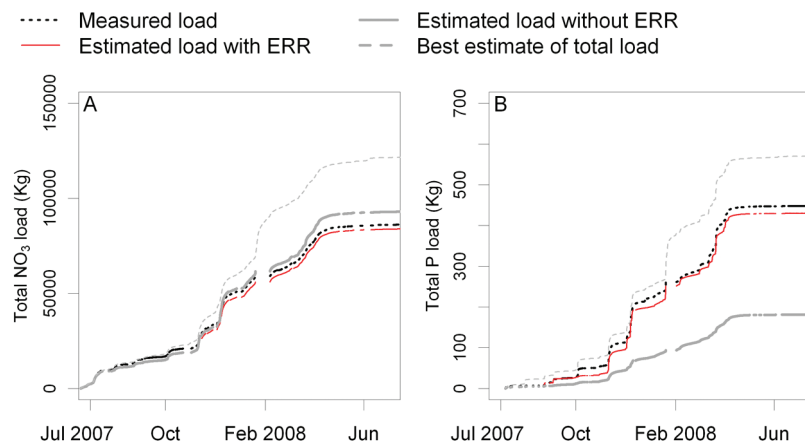

FIGURE 6. Measured and estimated annual NO$_3$ (A) and P (B) loads.

measurements of precipitation, discharge, and groundwater levels. Another innovative key element was our quantification of the concentration responses to individual events, whereas previous studies primarily used long-term concentration-discharge relations for their attempts to improve load estimates (*8, 9*). The short concentration changes during individual events are not captured by common low-frequency grab sampling, while they have a relatively large effect on total solute loads due to the simultaneous increase of the discharge.

In our research catchment, we found consistent and repetitive changes in NO$_3$ and P concentrations in response to rainfall events. The NO$_3$ concentrations dipped, while the P concentrations peaked during rainfall events throughout the year (Figure 3). For NO$_3$, similar responses to events were observed in comparable catchments by Poor and McDonnell (*10*), Borah et al. (*15*), and Chang and Carlson (*16*). The lowering of the NO$_3$ concentrations during rainfall events is related to the dilution of NO$_3$-rich stream discharge by NO$_3$-poor precipitation water. The short peaks in the P concentrations in response to events are also in correspondence with previous work in comparable catchments (*7, 13, 14*). These peaks were usually attributed to the flushing of particulate P during events. During dry periods, we observed large supplies of P-rich Fe- and Al-hydroxides accumulating at the ditch bottoms and inside tile drains in the Hupsel catchment. When the water flow velocities increased, this particulate P was detached and transported downstream (see also refs *7, 13,* and *14*). In many catchments, spatial aspects influence the water quality response to rainfall events at the catchment outlet. While relevant, these within-catchment

spatial variations were outside the scope of this paper. We refer to Kirchner et al. (*25*), Hopmans et al. (*26*), Lennartz et al. (*27*), and references therein for work related to spatially varying processes.

The consistent concentration response to rainfall events implies a strong connection between the dynamics in solute concentrations and the variations in quantitative hydrological variables like precipitation, discharge, and groundwater levels. This was confirmed by the results of our regression analyses. The singular regressions revealed many relations between the NO$_3$ and P event-response characteristics and the quantitative hydrological response characteristics (Figure S2). Furthermore, the event-response models from the sequential multiple linear regression analysis explained 74% up to 95% of the variance in the NO$_3$ and P response characteristics (see Table 2). These high coefficients of determination (R^2) supported our assumption that continuous quantitative hydrological data can be used for the prediction of the solute concentration response to rainfall events. The unexplained part of the variance in the NO$_3$ and P response characteristics can be attributed to uncertainties in the concentration measurements (*6*), nonlinearity of the relations, and possibly to seasonal changes in the concentration response to events. This seasonality in the hydrological conditions is covered by some of the explanatory variables (*APEI*, *Qs*, *QFs*, and *Gs*). Nevertheless, seasonality in temperature and land use also influences solute transport processes and might cause part of the unexplained variability in the NO$_3$ and P event-response characteristics.

We applied the event-response models to improve load estimates from low-frequency concentration data. Several

previous studies reported on the effects of low sampling frequencies on load estimates (e.g., refs *3−5*). In correspondence to this earlier work, our Figures 4b and 5b clearly demonstrated the large deviations between the interpolated weekly concentrations and the actual concentrations during rainfall events. These deviations severely propagate into the load calculations, due to the simultaneous high discharges. For load estimates based on low-frequency concentration data, this results in overestimates of the NO_3 loads (Figure 4c,d) and underestimates of the P loads (Figure 5c,d). The reconstruction of the concentration patterns using the event-response models produced much better load estimates, both for the validation period (Figures 4 and 5) and for the year-round measurements (Figure 6). In addition, we applied the response models to fill in the data gaps in the continuous water quality records. With this approach we produced the best estimates for the total yearly NO_3 and P loads of 121×10^3 kg (41 kg·ha^{-1}) and 570 kg (0.27 kg·ha^{-1}), respectively.

The results of this study demonstrate that using the explanatory strength of quantitative hydrological data can significantly improve load estimates. Our straightforward and transparent approach optimally combines the information about the concentration response to events from periods with frequent measurements with the information about long-term concentration patterns from low-frequency concentration data. Caution is required when extrapolating our event-response models to other time periods, other catchments or other solutes. For extrapolation purposes, a process-based modeling approach would be a more legitimate way to relate quantitative hydrological data to water quality dynamics and to deal with changed inputs and changed hydrological or hydrochemical conditions. Nevertheless, adequate water quality modeling is complicated and often requires many input variables that are only marginally known.

The presented approach can be applied to improve load estimates for all monitoring locations with consistent relations between the dynamics in solute concentrations and the variation in quantitative hydrological variables. In some catchments, however, biochemical or human-induced variations might dominate concentration dynamics and should be accounted for. This may require different types of explanatory information, such as temperature data or loads from industrial spills. For the Hupsel catchment, the high coefficients of determination (R^2) of our event-response models indicated that the dynamics in NO_3 and P concentrations are primarily driven by weather-induced hydrological variations.

In this paper we showed that regional water quality monitoring would benefit from frequent measurements during peak discharges obtained by in situ analyzers or storm event samplers. It would be expensive and laborious to install on-site equipment for continuous measurements at all sampling locations of a regional monitoring network. However, collecting continuous concentration data sets at representative locations during several events using a transportable field laboratory would be a valuable addition to a water quality monitoring network. The approach presented in this paper could then be applied to improve load estimates for periods without continuous measurements and for nearby monitoring locations in similar hydrological settings.

Acknowledgments

Supporting Information Available

Map with the location of the Hupsel catchment (Figure S1), detailed information on our field measurements (pp S3−S4), event characteristics for the selected rainfall events between June 2007 and July 2008 (Table S1), results of the singular linear regression analysis (Figure S2), and graphs with the measured versus the modeled NO_3 and P event-response characteristics, both for the selected rainfall events as well as for the events in the validation period (Figure S3). This material is available free of charge via the Internet at http://pubs.acs.org.

Literature Cited

(1) Oenema, O.; Oudendag, D.; Velthof, G. L. Nutrient losses from manure management in the European Union. *Livest. Sci.* **2007**, *112*, 261–272.

(2) EU. Council Directive of 23 October 2000 establishing a framework for Community action in the field of water policy. Directive number 2000/60/EC. Brussels.

(3) Kirchner, J. W.; Feng, X.; Neal, C.; Robson, A. J. The fine structure of water-quality dynamics: the (high-frequency) wave of the future. *Hydrol. Process.* **2004**, *18*, 1353–1359.

(4) Johnes, P. J. Uncertainties in annual riverine phosphorus load estimation: Impact of load estimation methodology, sampling frequency, baseflow index and catchment population density. *J. Hydrol.* **2007**, *332*, 241–258.

(5) Rozemeijer, J. C.; Van der Velde, Y.; De Jonge, H.; Van Geer, F. C.; Broers, H. P.; Bierkens, M. P. F. Application and evaluation of a new passive sampler for measuring average solute concentrations in a catchment-scale water quality monitoring study. *Environ. Sci. Technol.* **2010**, *44*, 1353–1359.

(6) Harmel, R. D.; Cooper, R. J.; Shade, R. M.; Haney, R. L.; Arnold, J. G. Cumulative uncertainty in measured streamflow and water quality data for small watersheds. *Trans. ASABE* **2006**, *49*, 689–701.

(7) Jordan, P.; Arnscheidt, A.; McGrogan, H.; McCormick, S. Characterizing phosphorus transfers in rural catchments using a continuous bank-side analyser. *Hydrol. Earth Syst. Sci.* **2007**, *11* (1), 372–381.

(8) Preston, S. D.; Bierman, V. J.; Silliman, S. E. An evaluation of Methods for the Estimation of Tributary Mass Loads. *Water Resour. Res.* **1989**, *25*, 1379–1389.

(9) Smart, T. S.; Hirst, D. J.; Elston, D. A. Methods for estimating loads transported by rivers. *Hydrol. Earth Syst. Sci.* **1999**, *3* (2), 295–303.

(10) Poor, C. J.; McDonnell, J. J. The effects of land use on stream nitrate dynamics. *J. Hydrol.* **2007**, *332*, 54–68.

(11) Jarvie, H. P.; Neal, C.; Smart, R.; Owen, R.; Fraser, D.; Forbes, I.; Wade, A. Use of continuous water quality records for hydrograph separation and to assess short-term variability and extremes in acidity and dissolved carbon dioxide for the River Dee, Scotland. *Sci. Total Environ.* **2001**, *265*, 85–98.

(12) Harris, G.; Heathwaite, A. L. Inadmissible evidence: knowledge and prediction in land and riverscapes. *J. Hydrol.* **2005**, *304*, 3–19.

(13) Stamm, C.; Flühler, H.; Gächter, R.; Leuenberger, J.; Wunderli, H. Preferential transport of phosphorus in drained grassland soils. *J. Environ. Qual.* **1998**, *27*, 515–522.

(14) Heathwaite, A. L.; Dils, R. M. Characterising phosphorus loss in surface and subsurface hydrological pathways. *Sci. Total Environ.* **2000**, *251−252*, 523–538.

(15) Borah, D. K.; Bera, M.; Shaw, S. Water, Sediment, Nutrient and Pesticide Measurements in an Agricultural Watershed in Illinois During Storm Events. *Trans. ASAE* **2003**, *46*, 657–674.

(16) Chang, H.; Carlson, T. N. Patterns of phosphorus and nitrate concentrations in small central Pennsylvania streams. *The Pennsylvania Geographer* **2004**, *42*, 61–74.

(17) Rozemeijer, J. C.; Broers, H. P. The groundwater contribution to surface water contamination in a region with intensive agricultural land use (Noord-Brabant, The Netherlands). *Environ. Pollut.* **2007**, *148*, 695–706.

(18) Wriedt, G.; Spindler, J.; Neef, T.; Meissner, R.; Rode, M. Groundwater dynamics and channel activity as major controls of in-stream nitrate concentrations in a lowland catchment system? *J. Hydrol.* **2007**, *343*, 154–168.

(19) Tiemeyer, B.; Lennartz, B.; Kahle, P. Analyzing nitrate losses from an artificially drained lowland catchment (North-Eastern Germany) with a mixing model. *Agric., Ecosyst. Environ.* **2008**, *123*, 125–136.

(20) Van der Velde, Y.; Rozemeijer, J. C.; De Rooij, G. H.; Van Geer, F. C.; Broers, H. P. Field-scale measurements for separation of catchment discharge into flow route contributions. *Vadose Zone J.* **2010**, *9*, 25–35.

(21) Fedora, M. A.; Beschta, R. I. Storm runoff simulation using an antecedent precipitation index (API) model. *J. Hydrol.* **1989**, *112*, 121–133.

(22) Makkink, G. F. Testing the Penman formula by means of lysimeters. *J. Inst. Water Eng.* **1957**, *11*, 277–288.

(23) Hewlett, J. D.; Hibbert, A. R. Moisture and energy conditions within a sloping soil mass during drainage. *J. Geophys. Res.* **1963**, *68*, 1081–1087.

(24) Cleveland, W. S. Robust locally weighted regression and smoothing scatterplots. *J. Am. Stat. Assoc.* **1979**, *74*, 829–836.

(25) Kirchner, J. W.; Feng, X.; Neal, C. Fractal stream chemistry and its implications for contaminant transport in catchments. *Nature* **2000**, *403*, 524–527.

(26) Corwin, D. L.; Hopmans, J.; De Rooij, G. H. From Field- to Landscape-Scale Vadose Zone Processes: Scale Issues, Modeling, and Monitoring. *Vadose Zone J.* **2006**, *5*, 129–139.

(27) Lennartz, B.; Tiemeyer, B.; Rooij, G.; Doležal, F. Artificially Drained Catchments-From Monitoring Studies towards Management Approaches. *Vadose Zone J.* **2010**, *9*, 1–3.